Table S2: number of neighbor GSCs and total GSCs in the analyzed genotypes ("neighbor rescue assay"), related to Fig. 5.

#	Figure	Name on graph	Time point	Average	SEM	n	P
		Average number of neighbor GSCs					
1	5G	control; *nos>lacZ*	2 dpci	6.15	±0.28	26	
2	5G	control; *nos>lacZ*	14 dpci	4.89	±0.38	35	
3	5G	control; *nos>Dg*	2 dpci	5.46	±0.31	26	
4	5G	control; *nos>Dg*	14 dpci	4.48	±0.41	25	
5	5G	*chinmo*^{k13009}; *nos>lacZ*	2 dpci	4.88	±0.34	15	
6	5G	*chinmo*^{k13009}; *nos>lacZ*	14 dpci	2.70	±0.38	29	< 1 x 10^{-4} vs line 14 (Student's t-test)
7	5G	*chinmo*^{k13009}; *nos>Dg*	2 dpci	5.39	±0.47	13	
8	5G	*chinmo*^{k13009}; *nos>Dg*	14 dpci	4.83	±0.44	29	< 1 x 10^{-4} vs line 22 (Student's t-test)
		Average number of total GSCs					
9	5H	control; *nos>lacZ*	2 dpci	8.19	±0.28	26	
10	5H	control; *nos>lacZ*	14 dpci	7.49	±0.21	35	
11	5H	control; *nos>Dg*	2 dpci	7.58	±0.24	26	
12	5H	control; *nos>Dg*	14 dpci	8.20	±0.30	25	
13	5H	*chinmo*^{k13009}; *nos>lacZ*	2 dpci	6.78	±0.25	15	
14	5H	*chinmo*^{k13009}; *nos>lacZ*	14 dpci	5.78	±0.22	29	< 7 x 10^{-7} vs line 10 (Student's t-test)
15	5H	*chinmo*^{k13009}; *nos>Dg*	2 dpci	7.15	±0.32	13	
16	5H	*chinmo*^{k13009}; *nos>Dg*	14 dpci	6.72	±0.50	29	< 1 x 10^{-4} vs line 14 (Student's t-test)

Table S3: Allele inheritance, related to Fig. 6.

#	Figure	Father's genotype and age (dpci)	Allele inherited	Average	SEM	n	P
1	6D	*ubi-GFP/ chinmo+* (23 dpci)	*ubi-GFP*	50.61%	±3.08	590	
2	6D	*ubi-GFP/ chinmo+*	*chinmo+*	49.39%	±3.08	583	
3	6D	*ubi-GFP/ chinmo^{1}*	*ubi-GFP*	34.77%	±1.72	660	1.01×10^{-18} vs line1 (χ^2 test)
4	6D	*ubi-GFP/ chinmo^{1}*	*chinmo^{1}*	65.23%	±1.72	1267	1.01×10^{-18} vs line 2 (χ^2 test)
5	6D	*ubi-GFP/ chinmo^{k13009}*	*ubi-GFP*	41.31%	±2.90	465	3.42×10^{-7} vs line 1 (χ^2 test)
6	6D	*ubi-GFP/ chinmo^{k13009}*	*chinmo^{k13009}*	58.69%	±2.90	703	3.42×10^{-7} vs line 2 (χ^2 test)

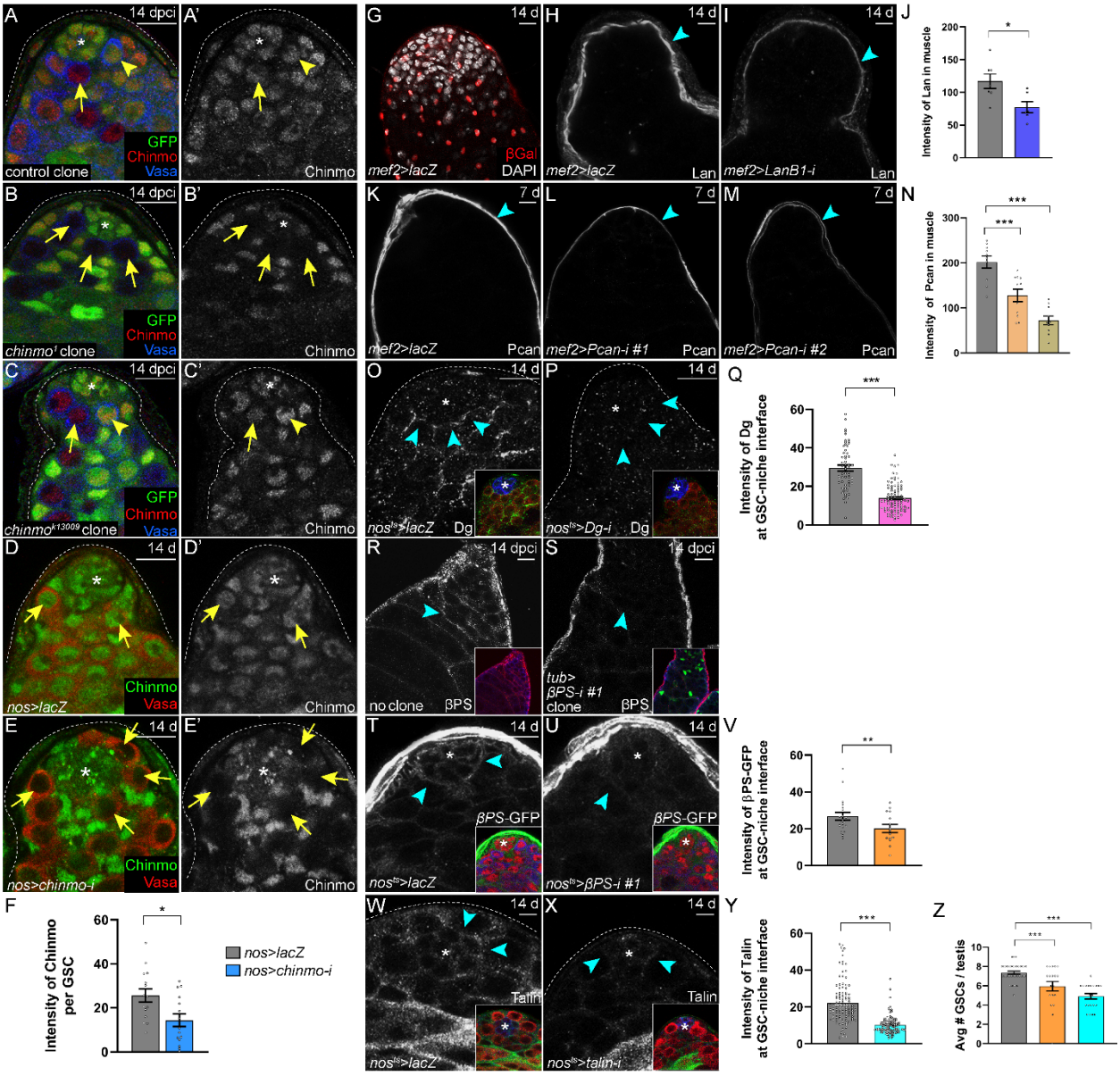

Figure S1: Characterization of *chinmo* alleles and validation of RNAi lines, related to Figs. 1-4

(A-C) Representative confocal images of Chinmo protein (red) in a control GSC clone (A-A', arrow), in *chinmo*^{1} GSC clones (B-B', arrow), and a *chinmo*^{k13009} GSC clone (C-C', arrow) at 14 dpci. Note similar expression of Chinmo in control clones and neighbor GSCs (A-C', arrow vs arrowhead, respectively). Note the absence of Chinmo in *chinmo*^{1} clones (B, arrows). Note the slight decrease in Chinmo in a *chinmo*^{k13009} clone compared to a neighbor GSC (C-C', arrow vs arrowhead, respectively). Clones are marked by the absence of GFP. Vasa (blue) marks germ cells. Clones are marked by arrows. Neighbors are marked by arrowheads.

(D-F) Representative confocal images of Chinmo protein (green) in GSCs (D, arrows) in a *nos>lacZ* control testes and in GSCs (E, arrows) in a *nos>chinmo*-RNAi testes in which *chinmo* is depleted from GSCs. The time point is 14 days. Graph (F) showing that Chinmo is significantly reduced in GSCs in *nos>chinmo*-RNAi testes (blue bar) compared to control *nos>lacZ* (gray bar). This establishes the efficacy of the *chinmo* RNAi line.
(G-J) Representative confocal images of a *mef2>lacZ* testis stained with βGal (red), illustrating that *mef2* is expressed only in muscle sheath cells (G). Lan (white) is expressed in the muscle of a control *mef2>lacZ* (H, arrowhead), and Lan protein is reduced when LanB1 is depleted from muscle cells (*mef2>LanB1-i*) (I, arrowhead). The time point is 14 days. (J) Graph showing that Lan is significantly reduced in *mef2>LanB1-i* testes (blue bar) compared to control *mef2>lacZ* testes (gray bar). This establishes the efficacy of the *LanB1* RNAi line.
(K-N) Representative confocal images of Pcan (white) in the muscle sheath of a control *mef2>lacZ* testis (K, arrowhead). Pcan protein is reduced when Pcan is depleted from muscle using two independent *Pcan*-RNAi lines (L,M, arrowhead). The time point is 7 days. (N) Graph showing the significant reduction of Pcan in *mef2>Pcan-i #1* (orange bar) or *mef2>Pcan-i #2* (brown bar) compared to *mef2>lacZ* testes (gray bar). This establishes the efficacy of the *Pcan* RNAi lines.
(O-Q) Dg (white) is expressed at low level at the GSC-niche interface in a control testis (O, arrowheads). Dg protein is reduced at this interface in a nos^{ts}*>Dg-i* testis (P, arrowheads). The insets in O,P show the testes stained with Dg (green), Vasa (red) and Fas3 (blue). The time point is 14 days. (Q) Graph showing that Dg is significantly reduced in nos^{ts}*>Dg-i* testes (pink bar) compared to control nos^{ts}*>lacZ* testes (gray bar). This establishes the efficacy of the *Dg* RNAi line.
(R-S) βPS integrin (white) is expressed on the somatic membranes in a WT testis (R). By contrast, βPS integrin is greatly reduced when most CySCs and cyst cells are positively-marked clones depleting βPS integrin (labeled *tub>βPS-i*) (S). Arrowhead in R,S indicates somatic membrane. The time point is 14 days (R) and 14 dpci (S). The insets in R,S show testes stained with GFP (green in S), βPS (red) and Vasa (blue). This establishes the efficacy of the *βPS* RNAi line.
(T-V) Expression of βPS-GFP integrin (white) at the GSC-niche interface in a control nos^{ts}*>lacZ* testis (T, arrowheads) is reduced in a nos^{ts}*>βPS-i* testis (U, arrowhead). The insets in T,U show testes stained with GFP (green), Chinmo (red) and Vasa (blue). (V) Graph shows significant reduction of βPS-GFP in nos^{ts}*>βPS-i* testes (orange bar) compared to control nos^{ts}*>lacZ* testes (gray bar).

(W-Y) Expression of Talin (white) at the GSC-niche interface in a control *nos^{ts}>lacZ* testis (W, arrowheads) is reduced in a *nos^{ts}>talin-i* testis (X, arrowheads). The insets in W,X show testes stained with Talin (green), Vasa (red) and Fas3 (blue). (Y) Graph shows significant reduction of Talin in *nos^{ts}>talin-i* testes (blue bar) compared to control *nos^{ts}>lacZ* testes (gray bar). This establishes the efficacy of the *talin* RNAi line.

(Z) Graph showing significant reduction in the number of GSCs when βPS (orange) or Talin (blue) is depleted from all GSCs (using *nos^{ts}-Gal4*).

Scale bar = 10 μM

In F,J,N,Q,V,Y,Z, error bars represent SEM.

* P ≤ 0.05; ** P ≤ 0.01; *** P ≤ 0.001 as assessed by Student's t-test (see STAR Methods).

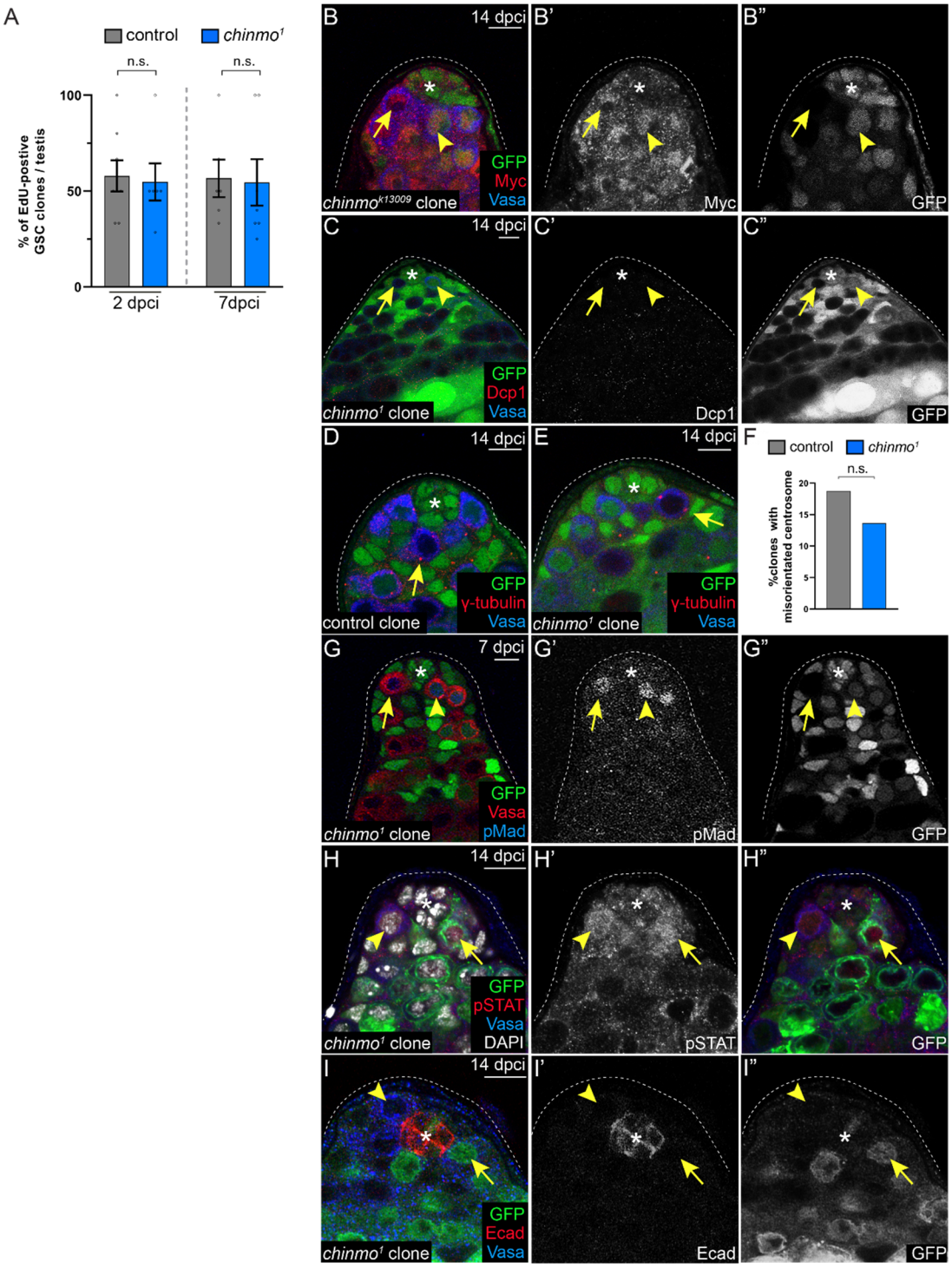

Figure S2: Known "winner" mechanisms are not observed in *chinmo*$^{-/-}$ GSCs, related to Fig. 2

(A) Graph of the percentage of GSC clones per testis in S phase as assessed by EdU incorporation at 2 and 7 dpci. There is no significant difference in S phase comparing control GSC clones (gray bars) to *chinmo*^{1}-mutant GSC clones (blue bars).

(B) A *chinmo*^{k13009} GSC clone (arrow) does not have increased expression of Myc (red) compared to a non-mutant GSC neighbor (arrowhead). Clones lack GFP. Vasa is blue. Time point is 14 dpci.
(C) A non-mutant neighbor GSC (arrowhead) does not apoptose as assessed by Dcp1 (red) in a testis with *chinmo*$^{-/-}$ GSC clones (arrow). Clones lack GFP. Vasa is blue. Time point is 14 dpci.
(D-F) Both a control GSC clone (D, arrow) and a *chinmo*^{1}-mutant GSC clone (E, arrow) have properly oriented centrosomes as assessed by γ-Tubulin (red). One centrosome is located at the GSC-niche interface and the other is at the opposite side of the GSC. Clones lack GFP. Vasa is blue. Time point is 14 dpci. (F) Graph showing that there is no significant difference in the percentage of mis-oriented centrosomes in control GSC clones (gray bar) and *chinmo*-mutant GSC clones (blue bar) at 14 dpci. Prior work has shown that ~20% of GSCs have mis-oriented centrosomes at 14 days of adulthood.
(G) Both a *chinmo*$^{-/-}$ GSC (arrow) and its non-mutant neighbor GSC (arrowhead) transduce BMP signals, as evidence by pMad (blue). Clones lack GFP. Vasa is blue. Time point is 7 dpci.
(H) Both a *chinmo*$^{-/-}$ GSC (arrow) and its non-mutant neighbor GSC (arrowhead) transduce Unpaired signals, as evidence by pSTAT (red). Clones are marked by membrane GFP. Vasa is blue. Time point is 14 dpci.
(I) Both a *chinmo*$^{-/-}$ GSC (arrow) and its non-mutant neighbor GSC (arrowhead) show E-Cad (red) enriched at the GSC-niche interface. Clones are marked by membrane GFP. Vasa is blue. Time point is 14 dpci.
Scale bar = 10 μM
In A, error bars represent SEM.
n.s. = not significant, as assessed by Student's t-test in A and by χ^2 test in F (see STAR Methods).

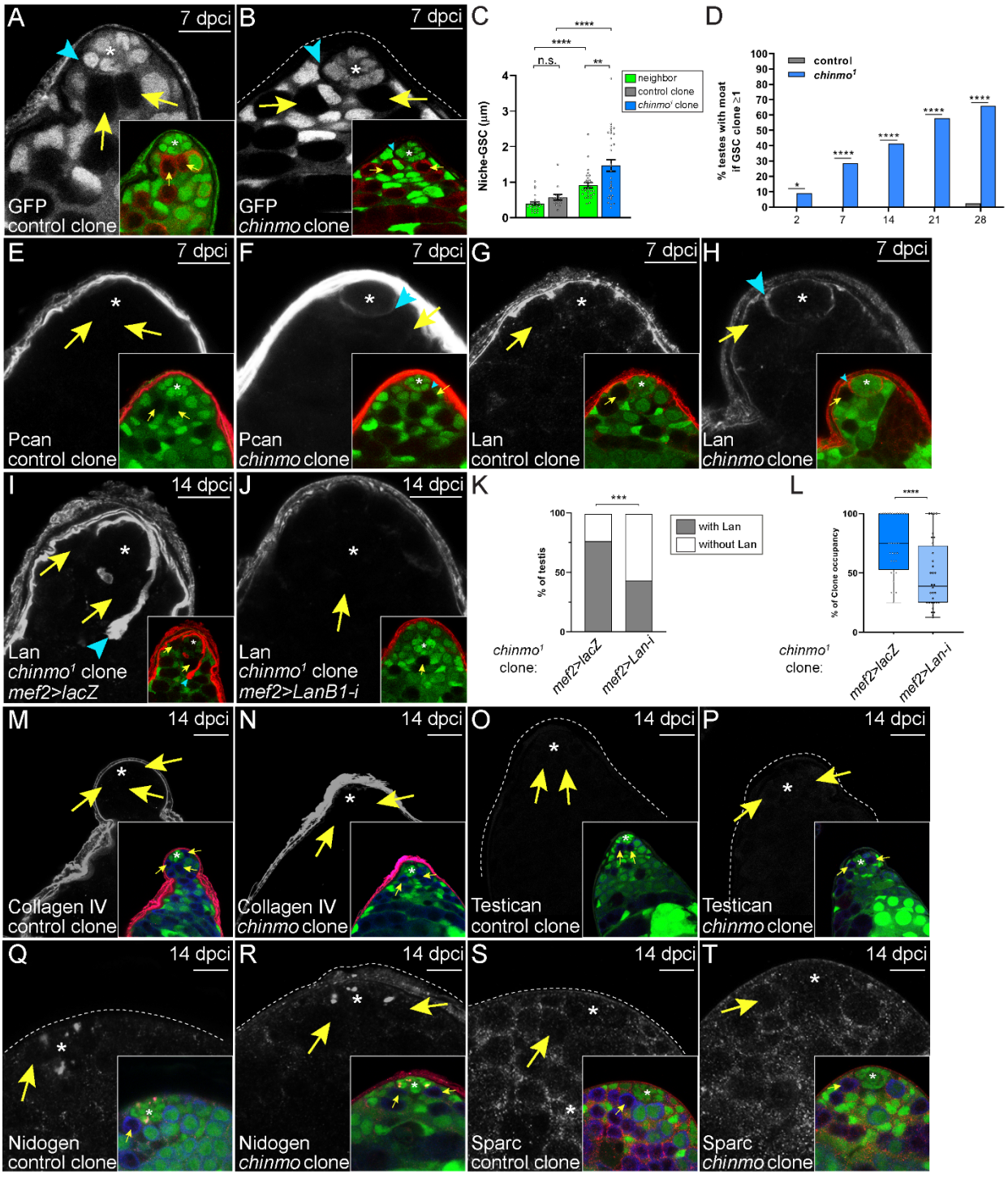

Figure S3: Additional characteristics of the moat, related to Fig. 3

(A-C) There is a gap between the niche and stem cells (B, arrowhead, quantified in C) in testes with *chinmo*$^{-/-}$ GSC clones but not in testes with control GSC clones (A, arrowhead, quantified in C). The clones in A,B are marked by arrows. Insets in A,B show the merged image in which clones lack GFP (green) and Vasa is red. (C) Graph showing the distance of each GSC to the

closest point of contact with niche cells in testes with control (gray circles) or *chinmo*$^{-/-}$ clones (blue circles). There is no significant difference in GSC-niche distance between control GSC clones (gray bar) and their GSC neighbors (first green bar). By contrast, *chinmo*$^{-/-}$ GSC clones (blue bar) are significantly farther from the niche than their GSC neighbors (second green bar). Additionally, *chinmo*$^{-/-}$ GSC clones (blue bar) are significantly farther from the niche than their control GSC clones (gray bar). Neighbors of *chinmo*$^{-/-}$ GSC clones (second green bar) are significantly farther from the niche than neighbors of control GSC clones (first green bar), presumably because of the moat in testes with *chinmo*$^{-/-}$ GSC clones.
(D) Graph showing percentage of testes with a "moat" around the niche if at least one GSC clone is present. There is a significant increase in testes with a moat when *chinmo*$^{-/-}$ clones (blue bars) are present and at every time point examined. Moats are rarely observed in testes with control clones (gray bars).
(E-F) Pcan (white) is observed in the moat as early as 7 dpci (F, arrowhead) when *chinmo*$^{-/-}$ clones (F, arrows) are present but not when control GSC clones (E, arrow) are. Insets show the merged image in which clones lack GFP (green), Pcan is red, and Vasa is blue.
(G-H) Lan (white) is observed in the moat as early as 7 dpci (H, arrowhead) when *chinmo*$^{-/-}$ clones (H, arrow) are present but not when control GSC clones (G, arrow) are. Insets show the merged image in which clones lack GFP (green), Lan is red, and Vasa is blue.
(I-L) Lan (white) is present in the moat in testes harboring *chinmo*^{1}-mutant GSC clones and mis-expressing a neutral protein lacZ in the muscle sheath (*mef2>lacZ)* (I). An arrowhead (I) marks a "tendril" of ectopic Lan in the testis lumen. By contrast, when Lan is depleted from the muscle sheath (*mef2>LanB1-i*), Lan expression in the moat is greatly reduced (J). Insets in I,J show the merged image in which clones lack GFP (green) and Lan is red. Time point is 14 dpci. (K) Graph shows the percentage of testes with Lan in the moat when *chinmo*^{1}-mutant clones are present and when the muscle sheath expresses a neutral protein (*mef2>lacZ*, first bar) or when the muscle is depleted for Lan (*mef2>LanB1-i*, second bar). (L) Clone occupancy of *chinmo*$^{-/-}$ clones is significantly reduced when Lan is depleted from the muscle sheath (light blue bar) compared to control (dark blue bar).
(M-N) Collagen IV (white) is not present in the moat in a testis harboring *chinmo*$^{-/-}$ clones (N). However, Collagen IV is expressed in the muscle BL in testes with control GSC clones (M) and with *chinmo*$^{-/-}$ clones (N). Clones are marked by arrows. Insets in M,N show the merged image in which clones lack GFP (green), Collagen IV is red, and Vasa is blue.

(O-P) Testican (white) is not expressed in testes with control GSC clones (O, arrows) or *chinmo*$^{-/-}$ clones (P, arrows). Insets in O,P show the merged image in which clones lack GFP (green), Testican is red, and Vasa is blue.
(Q-R) Nidogen (white) is not present in the moat in testes harboring *chinmo*$^{-/-}$ clones (Q, arrow). Nidogen is expressed in puncta in niche cells in testes with control (Q, arrow) or *chinmo*$^{-/-}$ GSC clones (R, arrow). Insets in Q,R show the merged image in which clones lack GFP (green), Nidogen is red, and Vasa is blue.
(S-T) Sparc (white) is not present in the moat in testes harboring *chinmo*$^{-/-}$ clones (T). Sparc is expressed at low levels in testes with control (S, arrow) or *chinmo*$^{-/-}$ GSC clones (T, arrow). Insets in S,T show the merged image in which clones lack GFP (green), Sparc is red, and Vasa is blue.
In M-T, testes were examined 14 dpci.
Scale bar = 10 μM
In C,L, error bars represent SEM.
** $P \leq 0.01$; *** $P \leq 0.001$; *** $P \leq 0.0001$; n.s. = not significant, as assessed by Student's t-test in C,L and by χ^2 test in D,K (see STAR Methods).

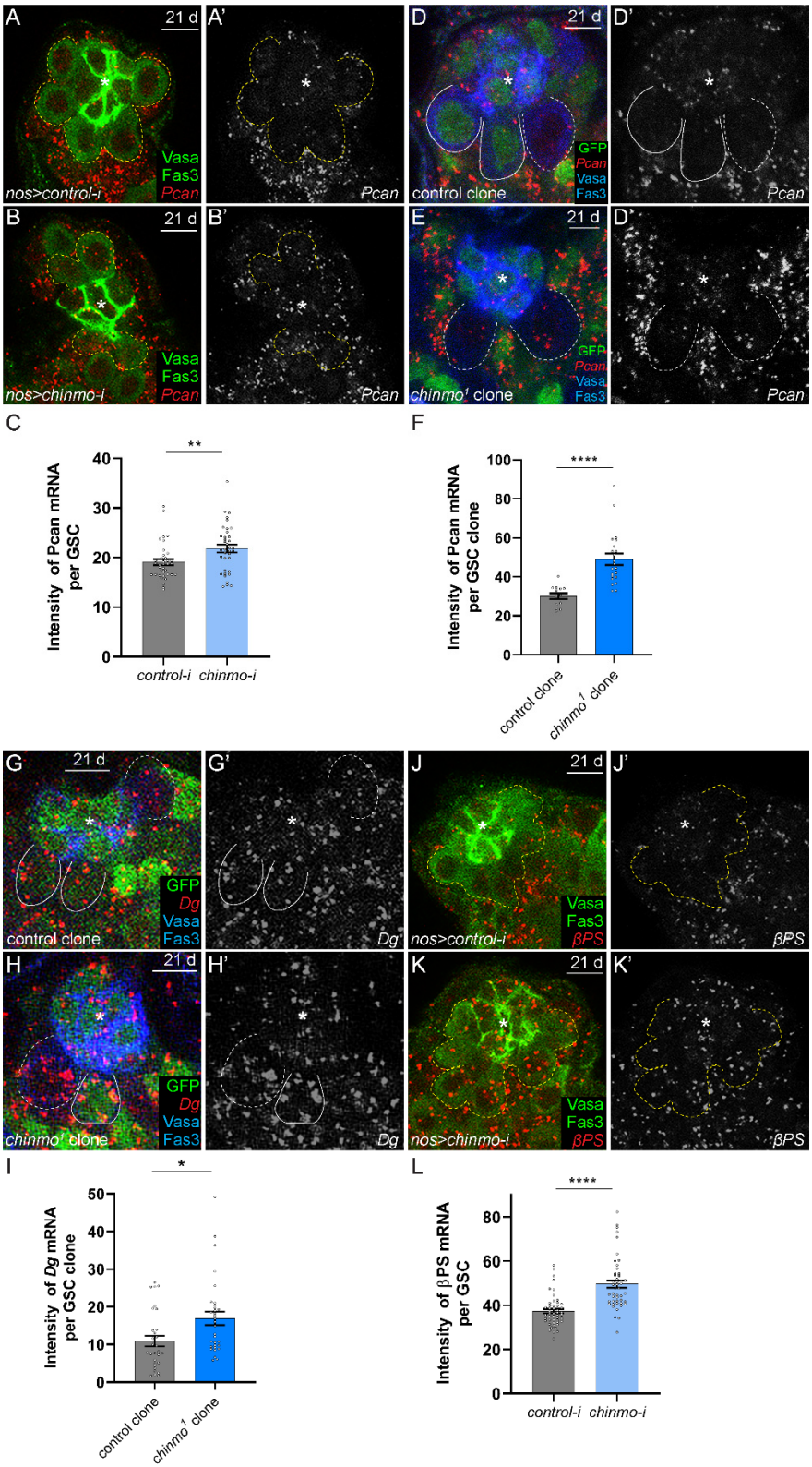

Figure S4: *Pcan*, *Dg*, and *βPS* integrin transcripts are increased in *chinmo*-deficient GSCs, related to Figs. 2 and 4.

(A-C) HCR-FISH for *Pcan* mRNA (red) in testes with GSCs (dashed line) expressing scrambled RNAi (labelled *nos>control-i*) (A) or with GSCs (dashed line) depleted for *chinmo* (labeled *nos>chinmo-i*) (B) for 21 days. (C) Graph showing that *Pcan* mRNA is significantly increased in GSCs depleted for *chinmo* (blue bar) compared to control GSCs (gray bar). Vasa (germ cells) and Fas3 (niche cells) are green.

(D-F) HCR-FISH for *Pcan* mRNA (red) in testes with control clones (dashed line) (D) or *chinmo*$^{-/-}$ clones (E) at 21 dpci. In D, the solid line outlines neighbor GSCs of control clones. (F) Graph showing that *Pcan* mRNA is significantly increased in *chinmo*$^{-/-}$ GSC clones (blue bar) compared to control GSC clones (gray bar). Clones lack GFP, and Vasa (germ cells) and Fas3 (niche cells) are blue.

(G-I) HCR-FISH for *Dg* mRNA (red) in testes with control clones (dashed line) (G) or *chinmo*$^{-/-}$ clones (H) at 21 dpci. In G,H, the solid line outlines neighbor GSCs. (I) Graph showing that *Dg* mRNA is significantly increased in *chinmo*$^{-/-}$ GSC clones (blue bar) compared to control GSC clones (gray bar). Clones lack GFP, and Vasa (germ cells) and Fas3 (niche cells) are blue.

(J-K) HCR-FISH for *βPS* mRNA (red) in testes with GSCs (dashed line) expressing scrambled RNAi (labelled *nos>control-i*) (J) or with GSCs (dashed line) depleted for *chinmo* (labeled *nos>chinmo-i*) (K) for 21 days. (L) Graph showing that *βPS* mRNA is significantly increased in GSCs depleted for *chinmo* (blue bar) compared to control GSCs (gray bar). Vasa (germ cells) and Fas3 (niche cells) are green.

Scale bar = 10 μM

In C,F,I,L, error bars represent SEM.

* $P \leq 0.05$; ** $P \leq 0.01$; **** $P \leq 0.0001$, as assessed by Student's t-test (see STAR Methods).

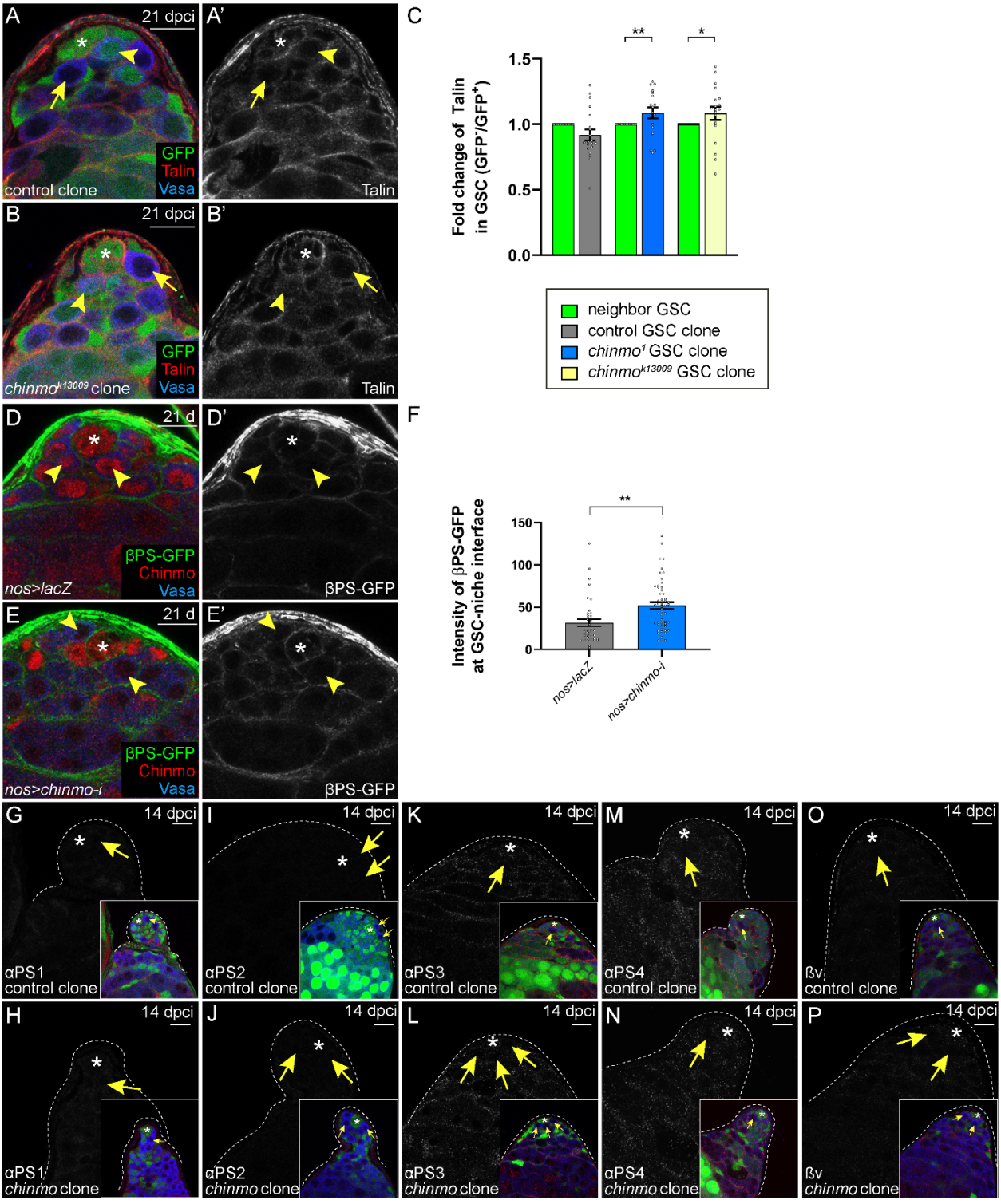

Figure S5: *chinmo*-mutant GSCs upregulate Talin and βPS integrin at the GSC-niche interface but not other integrin subunits, related to Fig. 4.

(A-C) Representative confocal images of Talin (red) in testes harboring control GSC clones (A,A', arrow) or *chinmo*^{k13009}-mutant GSC clones (B,B', arrow) at 21 dpci. Note the accumulation

of Talin at the GSC-niche interface in *chinmo*$^{-/-}$ GSCs (B', arrows) but not at that interface in control GSC clones (A', arrow) or at that interface in non-mutant neighbor GSCs (A',B', arrowheads). Clones lack GFP. Vasa is blue. (C) Graph showing the relative intensity of Talin at the GSC-niche interface. Talin is significantly higher in *chinmo*^{1}-mutant clones (blue bar) and *chinmo*^{k13009}-mutant clones (yellow bar) compared to neighbor GSCs (second and third green bars). A relative increase in Talin is not observed in control GSC clones (gray bar) compared to its neighbors (first green bar).

(D-F) Representative confocal images of control *nos>lacZ* testes (D) or testes in which *chinmo* was depleted from all GSC (*nos>chinmo-i*) (E) for 21 days. Note the increase in βPS at the GSC-niche interface when *chinmo* is depleted from all GSCs (E'). (F) Graph quantifying the intensity of βPS at the GSC-niche interface in control *nos>lacZ* testes (gray bar) or in testes in which GSCs are depleted for *chinmo* (blue bar). βPS at the GSC-niche interface is significantly higher in GSCs depleted for *chinmo* compared to controls.

(G-H) αPS1 (white) is expressed at very low levels in testes with control GSC clones (G) or *chinmo*^{1}-mutant clones (H).

(I-J) αPS2 (white) is expressed at very low levels in testes with control GSC clones (I) or *chinmo*^{1}-mutant clones (J).

(K-L) αPS3 (white) is expressed at low levels in testes with control GSC clones (K) or *chinmo*^{1}-mutant clones (L).

(M-N) αPS4 (white) is expressed at low levels in testes with control GSC clones (M) or *chinmo*^{1}-mutant clones (N).

(O-P) βv (white) is expressed at very low levels in testes with control GSC clones (O) or *chinmo*^{1}-mutant clones (P).

In G-P, clones are marked by arrows. Insets show merged image in which clones lack GFP and Vasa is blue. The time point is 14 dpci.

Scale bar = 10 μM

In C,F error bars represent SEM.

* $P \leq 0.05$; ** $P \leq 0.01$, as assessed by Student's t-test (see STAR Methods).

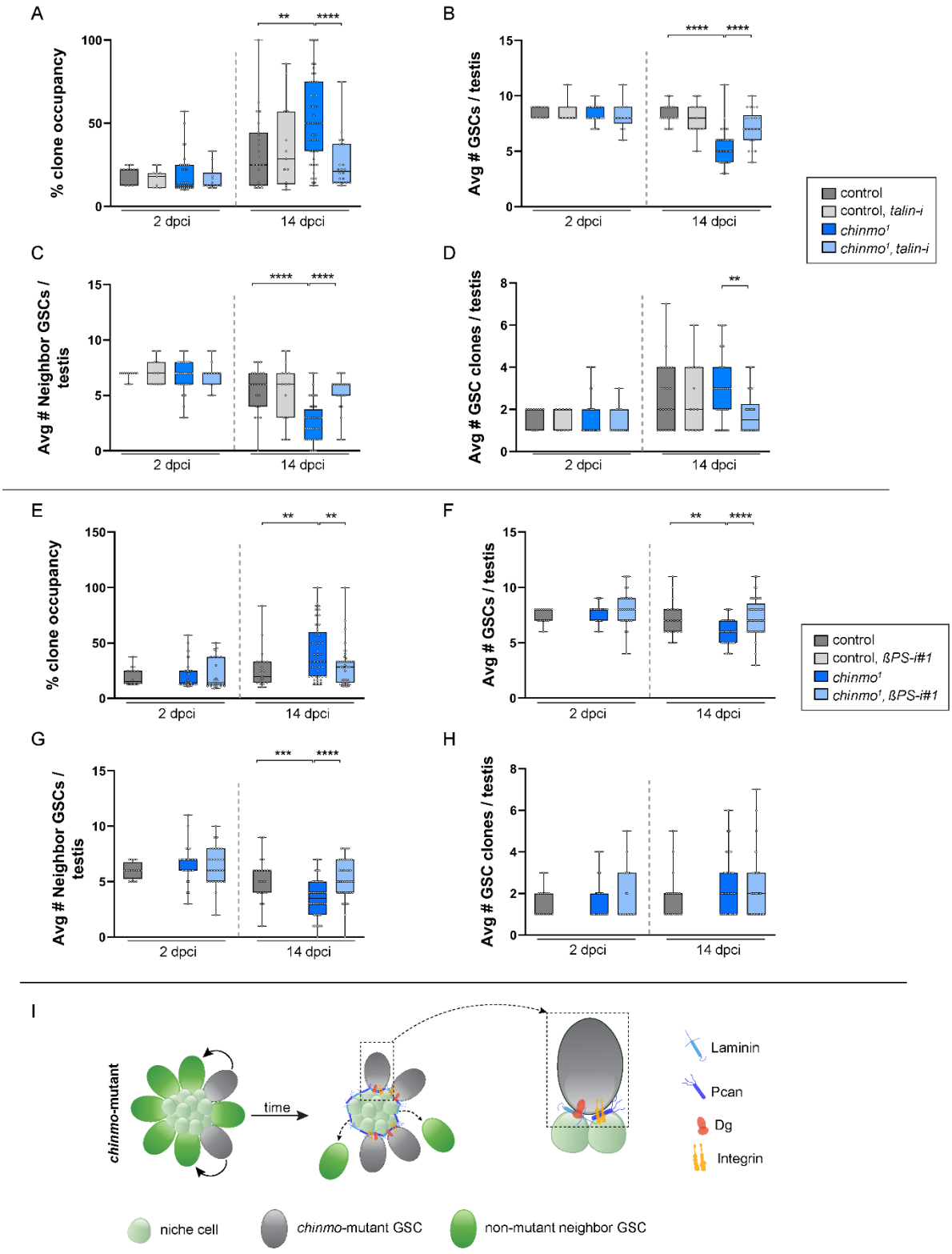

Figure S6: *chinmo*$^{-/-}$ GSCs require Talin and βPS integrin to remain in the altered niche, related to Fig. 4.

(A-D) Box and whisker plots showing clone occupancy (A), average total number of GSCs (B), average number of non-mutant GSC neighbors (C), and average number of GSC clones (D) in testes with control GSC clones (dark gray bars), with control GSC clones depleted for talin (light gray bars), with *chinmo*^{1}-mutant GSC clones (dark blue bars) or *chinmo*^{1}-mutant GSC clones depleted for Talin (light blue bars) at 2 and 14 dpci. *chinmo*$^{-/-}$ GSC clones have significantly increased clone occupancy at 14 dpci compared to control clones (A), and this increase is significantly reduced when Talin is depleted from the *chinmo*$^{-/-}$ clones (A). The average total number of GSCs (B) and the average number of non-mutant neighbors (C) are significantly decreased when *chinmo*$^{-/-}$ GSC clones are present, but this is reversed upon Talin depletion from the clones (B,C). Depletion of Talin from *chinmo*$^{-/-}$ GSC clones - but not from control GSC clones - reduced their ability to remain in the niche (D).

(E-H) Box and whisker plots showing clone occupancy (E), average total number of GSCs (F), average number of non-mutant GSC neighbors (G), and average number of GSC clones (H) in testes with control GSC clones (dark gray bars), with control GSC clones depleted for βPS (light gray bars), with *chinmo*^{1}-mutant GSC clones (dark blue bars) or *chinmo*^{1}-mutant GSC clones depleted for βPS (light blue bars) at 2 and 14 dpci. Note that control clones depleted for βPS are not recovered (H), suggesting that βPS is required for GSC maintenance. *chinmo*$^{-/-}$ GSCs have significantly increased clone occupancy at 14 dpci compared to control clones (E), and this is significantly reduced when βPS is depleted from the *chinmo*$^{-/-}$ clones (E). The average total number of GSCs (F) and the average number of non-mutant neighbors (G) are significantly decreased when *chinmo*$^{-/-}$ GSC clones are present, but this is reversed upon βPS depletion from the clones (F,G).

(I) Model: *chinmo*$^{-/-}$ GSC clones (gray cells) have increased expression of βPS integrin (yellow icon) at the GSC-niche interface, allowing them to remain in the resculpted niche. Boxed area enlarged at right illustrates a *chinmo*$^{-/-}$ GSC clone remaining in contact with the moat through increased localized expression of βPS integrin and Dg (orange icon, see Fig. 4H). By contrast, non-mutant neighbor GSCs (green stem cells in middle panel) do not have increased βPS expression at the GSC-niche interface and cannot remain long-term in the niche. The smaller, light green icons are niche cells.

In A-H, error bars represent SEM.

** $P \leq 0.01$; **** $P \leq 0.0001$, as assessed by Student's t-test (see STAR Methods).

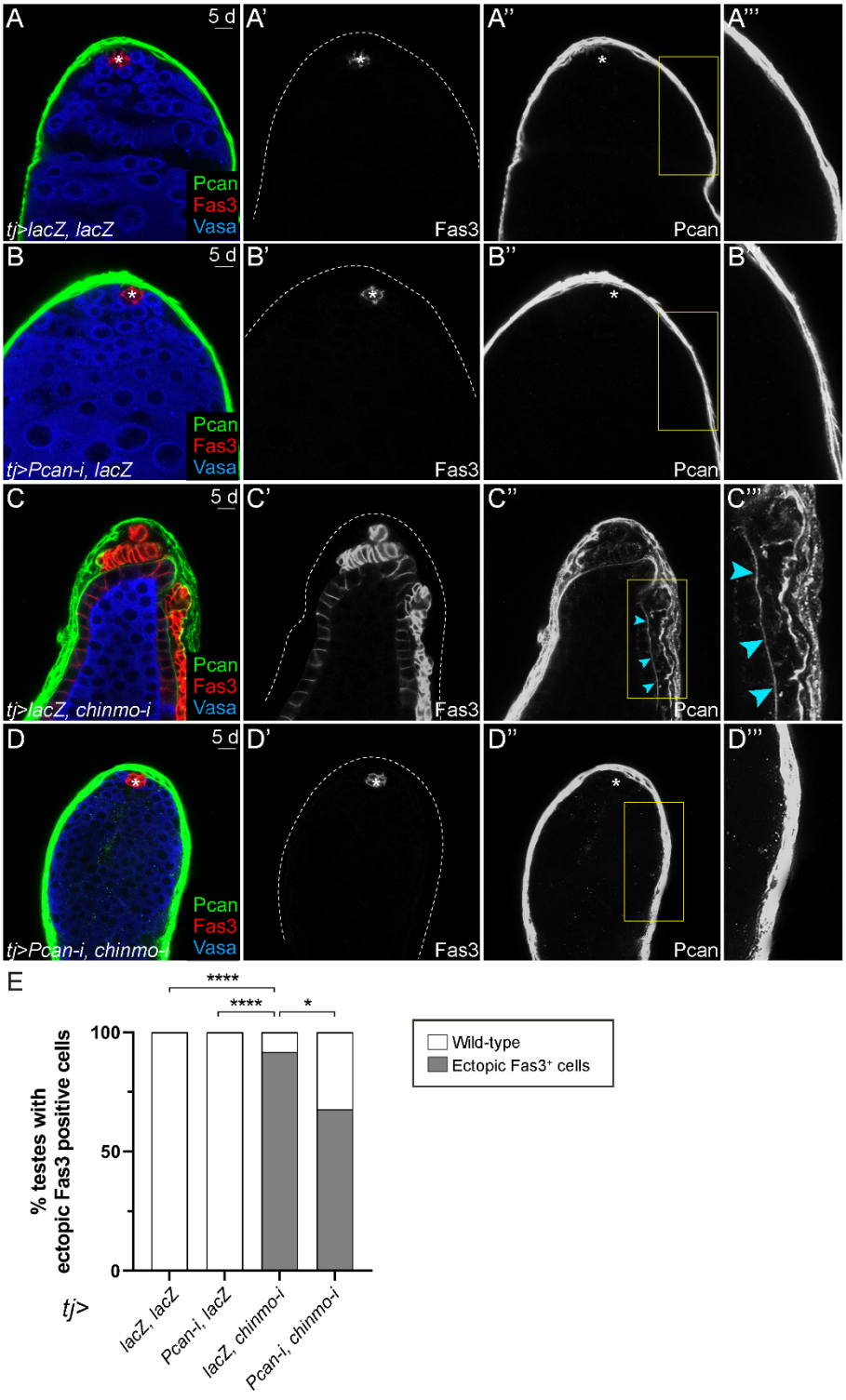

Figure S7: Pcan is ectopically expressed by CySCs lacking Chinmo, related to Figs. 2 and 3.

(A-D) Representative confocal images a showing a testis in which two neutral RNAi constructs (*UAS-lacZ*) are overexpressed in CySCs using the *tj-Gal4* driver labeled (*tj>lacZ, lacZ*) (A); a

testis in which Pcan is depleted from CySCs (labeled *tj>Pcan-i, lacZ*) (B); a testis in which Chinmo is depleted from CySCs (labeled *tj>lacZ, chinmo-i*) (C); a testis in which both Pcan and Chinmo are depleted from CySCs (labeled *tj>Pcan-i, chinmo-i*) (D). In control testes, Fas3 (red) is restricted to the niche (A, asterisk) and Pcan is restricted to the muscle BL. Depletion of Chinmo from CySCs causes a male-to-female sex transformation as evidenced by ectopic Fas3 (red) expression in all somatic cells (C'). Note the ectopic Pcan within the testis lumen in C"' (arrowheads), reminiscent of Pcan produced by ovarian follicle cells. This ectopic Pcan is caused by *chinmo*-depleted CySCs because when Pcan is concomitantly depleted, Pcan in the testis lumen is no longer observed (D"'). Additionally, co-depletion of Pcan and Chinmo from CySCs reduces the number of Fas3-positive sex-transformed cells (D). Time point is 5 days. Vasa is blue. The insets in A"'-D"' show enlargement of the muscle BL and Pcan (white).
(E) Graph showing the percentage of testes with sex-transformed somatic cells as evidenced by Fas3-positive cells outside of the niche at 5 days of adulthood. At this time point, most *tj>lacZ, chinmo-i* testes have a feminized soma. The percentage of testes with a feminized soma is significantly decreased when Pcan is depleted from *chinmo*-deficient CySCs (labeled *Pcan-i, chinmo-i*).
Scale bar = 10 μM
* $P \leq 0.05$; **** $P \leq 0.0001$, as assessed by χ^2 test (see STAR Methods).